Article

Boiling Heat Transfer Enhancement on Biphilic Surfaces

Evgeny A. Chinnov [1], Sergey Ya. Khmel [1], Victor Yu. Vladimirov [1,*], Aleksey I. Safonov [1] [ID], Vitaliy V. Semionov [1], Kirill A. Emelyanenko [2] [ID], Alexandre M. Emelyanenko [2] [ID] and Ludmila B. Boinovich [2]

[1] Kutateladze Institute of Thermophysics, Siberian Branch of the Russian Academy of Sciences, 1 Lavrentyev Ave., 630090 Novosibirsk, Russia

[2] A. N. Frumkin Institute of Physical Chemistry and Electrochemistry, Russian Academy of Sciences, Leninsky Prospect 31 Bldg. 4, 119071 Moscow, Russia

* Correspondence: victor.lipps@gmail.com; Tel.: +7-9137723236

Abstract: Flat surfaces with different patterns of hydrophobic spots were employed for experimental investigation of boiling heat transfer. In one case, hydrophobic spots were created on a smooth copper surface and on a surface coated with arrays of micrococoons from silicon oxide nanowires by vapor deposition of a fluoropolymer. In the second case, a hydrophobic coating was deposited on heater surfaces with cavity microstructures formed by laser ablation and chemisorption of fluorinated methoxysilane. Water under saturation conditions at atmospheric pressure was used as the working liquid. The temperature of the heating surface was varied from 100 to 125 °C, and the maximum value of the heat flux was 160 W/cm². Boiling heat transfer on the test biphilic surfaces was significantly (up to 600%) higher than on non-biphilic surfaces. Surface texture, the shape of hydrophobic regions, and the method of their creation tested in this study did not show a significant effect on heat transfer. The boiling heat transfer rate was found to depend on the size of hydrophobic spots, the distance between them, and hence the number of spots. The highest heat transfer efficiency was detected for the surface with the largest number of hydrophobic spots. After long-term experiments (up to 3 years), the heat transfer coefficient on the obtained surfaces remained higher than on the smooth copper surface. Biphilic surfaces with arrays of cavities formed by laser ablation turned out to be the most stable during prolonged contact with boiling water.

Keywords: wettability; biphilic; surface modification; boiling; heat transfer enhancement

1. Introduction

Boiling heat transfer makes it possible to remove high heat fluxes at low overheating of the heated surface relative to the saturated vapor temperature because of the high latent heat of the phase transition. Boiling is widely used to cool electronic devices, nuclear reactors, electric power generators, etc. Biphilic surfaces can be suitable for cooling smooth surfaces of chips and optical devices of high-power lasers.

Boiling is a complex process that depends on many factors, in particular, the roughness (structure) and wettability of the surface on which this process occurs. Recently, there has been an increase in boiling studies associated with the development of new micro/nano surface modification techniques that provide heat transfer enhancement [1–7]. Micro/nano modification includes both micro/nano surface structuring and application of thin coatings (nanocoatings). Both approaches change the physicochemical properties of boiling surfaces, in particular, wettability.

It is known that nucleate boiling begins earlier on hydrophobic surfaces than on hydrophilic surfaces because hydrophobic surfaces have more centers of vapor bubble nucleation. This is due to the higher gas concentration in submicron cavities on hydrophobic surfaces; in addition, after bubble detachment, a larger amount of vapor remains on hydrophobic surfaces compared to hydrophilic surfaces [8]. As a result, at low heat fluxes, the boiling heat transfer coefficient on a hydrophobic surface is higher than on a hydrophilic

surface. With an increase in the heat flux, the number of bubbles increases and they begin to coalesce, which prevents liquid access to the surface and deteriorates heat transfer, leading to the appearance of dry spots and, ultimately, to a boiling crisis. Boiling on hydrophilic surfaces starts later than on hydrophobic surfaces; however, at increased heat fluxes, the boiling heat transfer coefficient of hydrophilic surfaces is higher due to good surface wettability, leading to an enhanced liquid supply to the surface. For the same reason, the critical heat flux is higher. Thus, the use of hydrophobic surfaces is preferred at low heat fluxes, and the use of hydrophilic surfaces at high heat fluxes.

Several approaches have been proposed to simultaneously utilize the advantages of both types of surfaces in boiling processes. One approach is to use surfaces with mixed (heterogeneous, patterned) wettability or biphilic surfaces. Although this approach has been proposed previously [9,10], increased interest of researchers in the effect of biphilic surfaces on pool boiling heat transfer enhancement arose after the publication of a study [11] in 2010. Apparently, this is due to the above-mentioned development of new micro/nano surface modification techniques. These techniques emerged primarily in microelectronics and MEMS and were developed for silicon. Therefore, a significant part of the studies of biphilic surfaces was carried out on silicon substrates [8,11–14]. Hydrophilic surfaces were obtained, as a rule, by oxidation of silicon substrates [8,11–14]. Hydrophobic surfaces were obtained by applying a fluoropolymer coating using the spin-coating method [11–14]. Particle deposition can be analyzed using the method presented in [15]. Surface patterns were made by photolithography.

Pool boiling experiments have shown [11] an increase in both the heat transfer coefficient and the critical heat flux on surfaces with hydrophobic spots (regions) located on a hydrophilic background (surrounding) surface. Apparently, a large number of vaporization centers are formed on the hydrophobic surface of the spots, which provides rapid boiling at low overheating and a high heat transfer coefficient. In turn, the background hydrophilic surface between hydrophobic spots prevents bubble coalescence and increases the critical heat flux. In addition, the liquid and vapor flows are separated, which facilitates liquid access to the surface and contributes to an increase in the critical heat flux. Regular hexagonal spots were formed at the nodes of a uniform square lattice. The distance between the centers of the spots (pitch) was varied from 50 to 200 μm, and the size of hydrophobic spots was 40–60% of this distance.

Jo et al. [12] also investigated pool boiling heat transfer on biphilic surfaces consisting of hydrophobic spots patterned on a hydrophilic background surface. The effect of the hydrophobic spot size (50–500 μm), spot pitch (0.5 and 1 mm), and the number of hydrophobic spots (150 and 600) was studied. It has been shown that at low heat fluxes (<30 W/cm^2), the heat transfer coefficient is determined by the size of hydrophobic spots and the distance between them. At high heat fluxes, it is determined by the number of spots and their size. It is argued that the area ratio (the ratio of the total hydrophobic surface area to the total boiling area) has little effect on the heat transfer coefficient.

It is known that surface roughness has a significant effect on wettability; in particular, an increase in roughness leads to an increase in both the hydrophilicity of hydrophilic surfaces and the hydrophobicity of hydrophobic surfaces [10,16]. Betz et al. [13] used this circumstance to create biphilic surfaces with a maximum wettability gradient. Superbiphilic surfaces exhibited exceptional pool boiling performance with high critical heat fluxes (>100 W/cm^2) and very high heat transfer coefficients (10 W/cm^2 K). In particular, this coefficient was more than twice the heat transfer coefficient for biphilic surfaces with contact angles of 20° and 120°.

Jo et al. [14] systematically studied the dependences of the critical heat flux and boiling heat transfer on biphilic surfaces on the size and number of hydrophobic dots, pitch, and area ratio. It was found that the critical heat flux is inversely proportional to the area ratio and reaches maximum values for small values of this ratio. Boiling heat transfer depends on the size and number of hydrophobic dots and the pitch between them, but weakly depends on the area ratio. Therefore, for a significant enhancement of pool boiling heat

transfer, a biphilic surface should contain a large number of hydrophobic dots 50–100 μm in size and at the same time should have a relatively small total hydrophobic area.

Motezakker et al. [8] studied boiling parameters on biphilic surfaces for different area ratios. Maximum values of the critical heat flux and the heat transfer coefficient were achieved at an area ratio of 38.46%, which corresponded to a hydrophilic spot diameter of 700 μm.

Other common materials used to fabricate substrates (heaters) when creating biphilic surfaces are metals and, above all, copper [17–21]. In this case, the hydrophilic surface was a metal surface or a thin film of another material deposited on metal. Hydrophobic surfaces were obtained by applying a fluoropolymer coating or silicone. Surface patterns were made by photolithography or other methods using a mask.

Takata et al. [17] created two types of biphilic surfaces: in one case, superhydrophobic spots of a nickel–fluoropolymer composite were deposited on a clean copper surface; in the other case, fluoropolymer spots were deposited on a superhydrophilic surface of titanium oxide deposited on a copper surface. In both cases, an enhancement of water pool boiling heat transfer was achieved. The determining parameters were the hydrophobic spot size and the area ratio. It was shown that a decrease in the spot size at a constant pitch leads to an increase in the heat transfer coefficient. For the same area ratio, the heat transfer coefficient was the same regardless of the type of coating, the shape of spots, etc. The best results were obtained for surfaces with minimum spot size and area ratio.

In a study [18], hydrophobic spots were formed from a nickel–fluoropolymer composite on a copper surface. The heat transfer coefficient was shown to be higher for smaller spot diameters and smaller pitches between spots.

The authors of [19,20] applied an original approach to the fabrication of biphilic surfaces aimed at minimizing their production cost. Hydrophobic spots and stripes were formed by spreading a high-temperature silicone sealant on a copper surface through a template. The spots were 2 and 4 mm in size with a pitch of 6 mm. Boiling heat transfer enhancement was obtained, with the enhancement being higher on spots of smaller diameter. However, the aging problem for such surfaces was not discussed in these papers.

Može et al. [21] created superbiphilic surfaces on an aluminum surface. Superhydrophobic spots were produced by CVD deposition of fluorinated silane on a nanostructured metal surface, and a superhydrophilic background (surrounding) surface was obtained by laser texturing. The heat transfer was found to significantly depend on the pitch and area ratio but weakly on the spot size. The maximum heat transfer coefficient was obtained for a superbiphilic surface with a spot size of 0.5 mm, a pitch of 1 mm, and an area ratio of 23%.

Promising methods for producing biphilic surfaces are laser techniques. These methods use beams with a minimum diameter of tens of microns. Therefore, a biphilic pattern for heat transfer enhancement can be easily achieved by scanning a substrate without using photolithography or other mask techniques. This approach was employed in [21,22], where certain surface areas were laser textured to obtain a biphilic pattern, and in [23], the wettability of the applied coating was changed by laser beam heating, resulting in a biphilic pattern.

Thus, experiments with silicon, aluminum, and copper substrates (heaters) have shown that the use of biphilic surfaces consisting of hydrophobic spots on a hydrophilic background surface leads to an enhancement of pool boiling heat transfer. Most studies have been performed on silicon substrates; studies on metal substrates, e.g., copper substrates, are markedly fewer in number. In particular, metal substrates with small hydrophobic spot sizes (less than 250 μm) have not been investigated, although it follows from the literature that the heat transfer enhancement is greater for smaller spot sizes. At the same time, the findings of the previous studies are contradictory: for example, in [12,14], it is stated that the heat transfer coefficient (HTC) depends weakly on the area ratio, whereas in [8,21], the optimal values of the area ratio are given, but they are different: 38.46% and 23%, respectively. We also note that the aging problem is not considered in

papers on biphilic surfaces, although it is fundamental, as for any micro/nanomodified surface [24,25]. Further improvement in boiling heat transfer on biphilic surfaces can be achieved by preliminary micro/nanostructuring [8,13,26]; in particular, laser methods are promising for micro/nanostructuring [21]. New interesting approaches to enhancing boiling heat transfer have also been proposed—for example, the simultaneous use of a biphilic surface and nanofluids. [27].

In this paper, we present the results of a study of pool boiling heat transfer on biphilic copper surfaces with small hydrophobic spots. Spots of different shapes with an equivalent diameter of 50 to 100 μm were used. Boiling was investigated on three types of such surfaces with different micro/nanostructuring (micro/nanotexturing): a smooth copper surface, a copper surface coated with micro/nanostructures in the form of arrays of micrococoons from silicon oxide nanowires, and a copper surface with cavity microstructures formed by laser ablation. In addition, long-term experiments were carried out to study the problem of aging of biphilic surfaces.

2. Materials and Methods

2.1. Biphilic Surfaces and Their Fabrication Process

In this work, we used copper heaters with surface texture of three types: a smooth surface, a surface with micro/nanostructures in the form of arrays of micrococoons from silicon oxide nanowires, and a surface with arrays of microcavities formed by laser ablation. Heaters with biphilic surfaces were fabricated by two methods. In one method, a fluoropolymer coating was applied to the surface of heaters of the first and second types through a mask using hot wire chemical vapor deposition (HWCVD) with the formation of hydrophobic spots. In the other method, a hydrophobic coating was applied to the surface of heaters of the third type by chemisorption of fluorinated methoxysilane from the vapor phase at a temperature of 100–110 °C [28,29]. Detailed information on the characteristics of the surfaces used is given in Table 1.

Table 1. Characteristics of the surfaces used.

Surface Number	Type of Surface Texture	Hydrophobic Coating	Shape and Size of Hydrophobic Spots	Spot Pitch and Number of Spots	Area Ratio
1	Micrococoons from SiOx nanowires	No	No	No	0
2	Micrococoons from SiOx nanowires	Fluoropolymer HWCVD	0.1 mm diameter circle	0.5 mm, 69	2.8%
3	Micrococoons from nanowires SiOx	Fluoropolymer HWCVD	0.1 mm diameter circle	0.5 mm, 69	2.8%
4	Smooth copper surface	Fluoropolymer HWCVD	0.1 mm diameter circle	0.5 mm, 69	2.8%
5	Micrococoons from SiOx nanowires	Fluoropolymer HWCVD	0.05 mm diameter circle	0.2 mm, 506	5.1%
6	Smooth copper surface	Fluoropolymer HWCVD	0.05 mm diameter circle	0.2 mm, 506	5.1%
7	Copper surface with an array of cavities formed by laser ablation	Hydrophobization by chemisorption of fluorinated methoxysilane	Triangular cross-section cavity with an effective diameter of 0.07 mm	0.78 mm, 32	2.1%
8	Copper surface with an array of cavities formed by laser ablation	Hydrophobization by chemisorption of fluorinated methoxysilane	Rectangular cross-section cavity with an effective size of 0.1 mm	0.78 mm, 32	3.4%

A detailed description of the HWCVD for a fluoropolymer coating is given in [30,31]. We used two masks made of stainless steel with holes 50 μm and 100 μm in diameter located at the nodes of a square lattice with a pitch (distance between the centers of the holes) of 200 μm and 500 μm, respectively. These masks were tightly pressed against the heater surface during the deposition of the fluoropolymer coating. As a result, round hydrophobic spots 50 μm in diameter with a pitch of 200 μm and 100 μm in diameter with a pitch of 500 μm were formed on a smooth copper surface.

The second type of surface texture was obtained using arrays of micrococoons from silicon oxide nanowires. A micrococoon is a submicron-sized tin catalyst particle covered on all sides with silicon oxide nanowires. Tin catalyst particles were formed from a tin island film deposited by vacuum thermal evaporation. Before the deposition of tin, the copper heater surface was coated with a barrier layer of tungsten about 100 nm thick. Silicon oxide nanowires on tin catalyst particles were synthesized by gas-jet electron beam plasma chemical vapor deposition. The procedure for synthesizing arrays of micrococoons from SiO_x nanowires on copper heater surfaces is described in detail in [25]. SiO_x was chosen for the synthesis due to its high chemical and thermal stability. Such micro/nanostructures show the greatest resistance to destruction by boiling compared to other structures [25,31]. Figure 1a shows the surface morphology with arrays of micrococoons from silicon oxide nanowires before the deposition of the hydrophobic layer (fluoropolymer film). In Table 1, this surface is numbered 3.
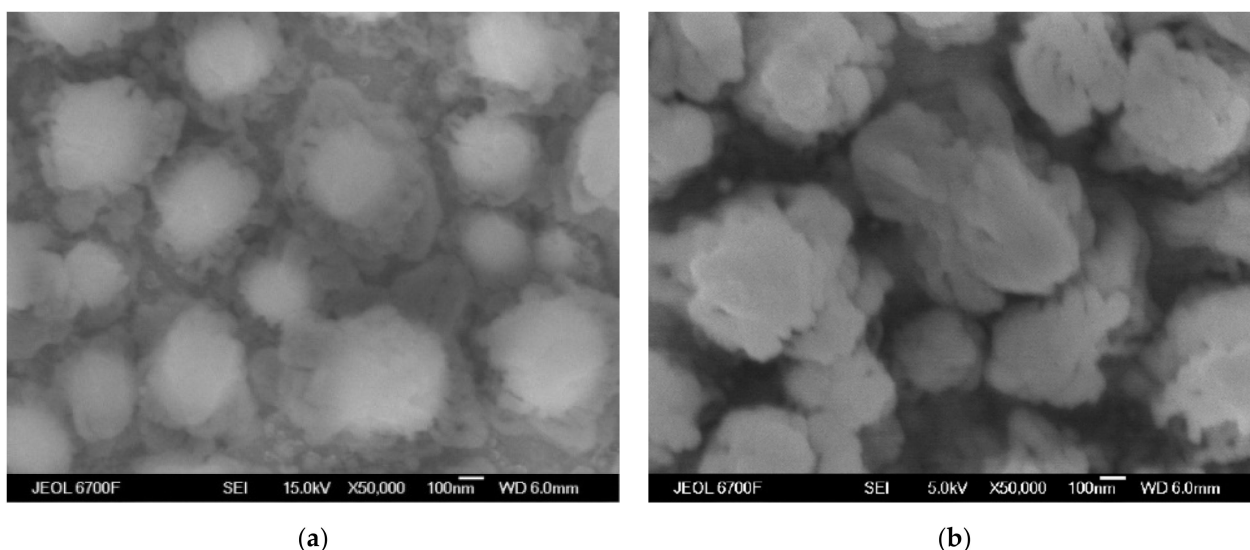

Figure 1. Surface morphology No. 3 before (**a**) and after the deposition of fluoropolymer (**b**).

Fluoropolymer film was deposited on these heaters by HWCVD, as in the previous case, using the same masks and under the same conditions. As a result, round hydrophobic spots 50 μm in diameter with a pitch of 200 μm and 100 μm in diameter with a pitch of 500 μm were formed on the copper heater surface with arrays of micrococoons. Figure 1b shows the surface morphology with arrays of micrococoons after the deposition of the fluoropolymer film. Features of the formation of hydrophobic spots on arrays of micrococoons from silicon oxide nanowires are given in [32]. Figure 2 shows SEM images at different magnifications of the surface after the deposition of fluoropolymer spots. It can be seen that the deposition through the mask results in round fluoropolymer spots.
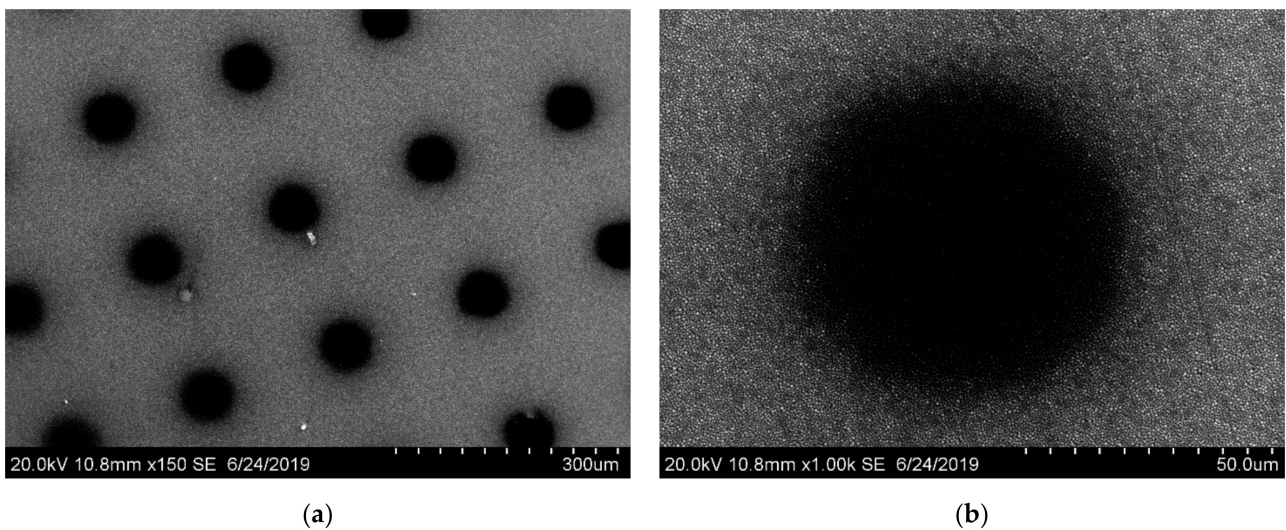
(**a**)   (**b**)

Figure 2. SEM images of surface No. 5 after the deposition of the fluoropolymer coating through a 50–200 μm mask (hole diameter 50 μm, pitch 200 μm): (**a**) magnification 150, scale bar 300 μm, (**b**) magnification 1000, scale bar 50 μm.

The elemental composition of these coatings was analyzed by EDS. Figure 3 shows surface mapping images for different elements. Fluorine and carbon (fluoropolymer components) are clearly detected in the region of spots (Figure 3a,b), and silicon dominates in the region between the spots (Figure 3c). This confirms that the composition of the spots corresponds to the fluoropolymer and that there is no fluoropolymer in the space between the spots.
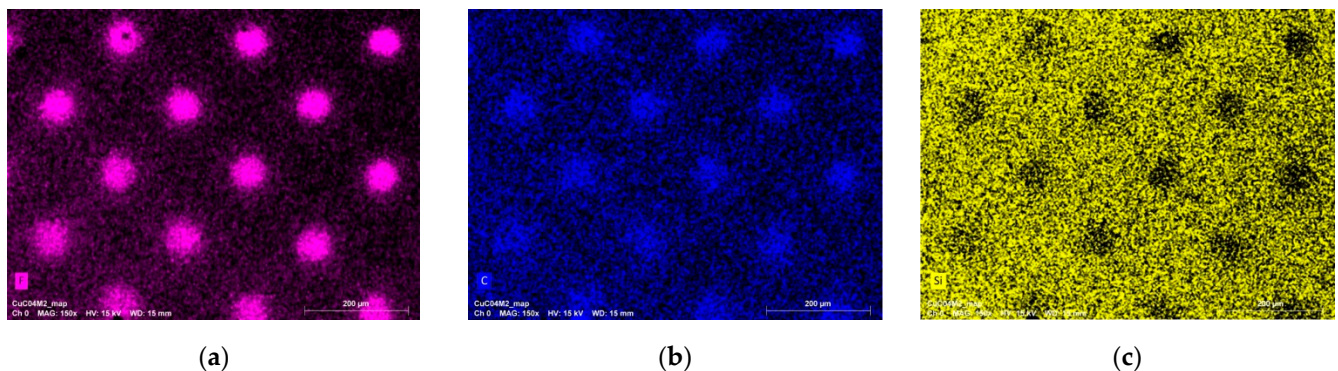

(**a**)   (**b**)   (**c**)

Figure 3. Elemental composition map of the biphilic heater surface obtained using a 50–200 μm mask: (**a**) fluorine, (**b**) carbon, and (**c**) silicon. Scale bar: 200 μm.

The third type of surface texture was obtained by laser ablation with the formation of arrays of cavities with an equivalent diameter of about 70–100 μm on the boiling surface. For texturing, we used an Argent-M laser marking system (Laser Technology Center, Russia) based on an infrared ytterbium fiber laser with a wavelength of 1.064 μm, a focused laser spot diameter (at the 1/e2 level) of 40 μm, and a peak power of up to 0.95 mJ in TEM00 mode. Local surface regions were subjected to a single or multiple laser treatment with a pulse duration of 200 ns and a pulse frequency of 20 kHz. Surfaces with arrays of cavities were fabricated. In the single pass mode, 1568 pulses were used to fabricate one cavity and the resulting cavities had a triangular cross section. In the multiple pass mode, 7840 pulses were used and rectangular cross-section cavities were obtained. Figure 4 shows images of individual triangular and rectangular cavities.
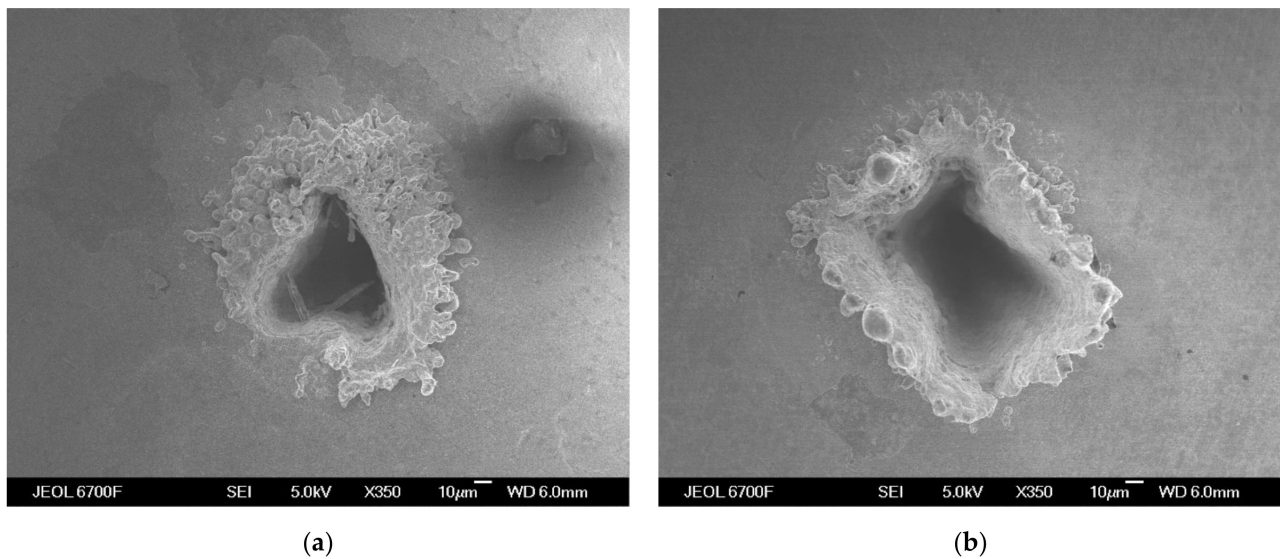
Figure 4. SEM image of an individual cavity on surface No. 7 (**a**) and surface No. 8 (**b**). Scale bar: 10 μm.

The cross-section of the triangular cavity has an equivalent diameter of about 70 μm, and the cross-section of the rectangular cavity has an approximate size of 100 μm. For both surfaces, the pitch was 780 μm. To create biphilic surfaces, copper surfaces were hydrophobized by UV/ozone activation, followed by chemisorption of fluorinated methoxysilane from the vapor phase at a temperature of 100–110 °C. This resulted in the formation of a layer of two-dimensional chemically cross-linked fluoroxysilane which is bonded through hydroxyl groups to the surface at ablation sites [28,29]. It was expected that the hydrophobized layer on the smooth copper surface would be quickly destroyed, whereas in laser-treated areas it will remain for a long time. The main factor in this process should be different types of adsorption of fluoroxysilane molecules: stronger chemical adsorption in laser-treated areas and less strong physical adsorption in untreated areas. Thus, a biphilic surface is formed.

Figure 5 shows SEM images at different magnifications of the side wall of the rectangular cavity. It can be seen that the laser-treated surface becomes rough and porous.
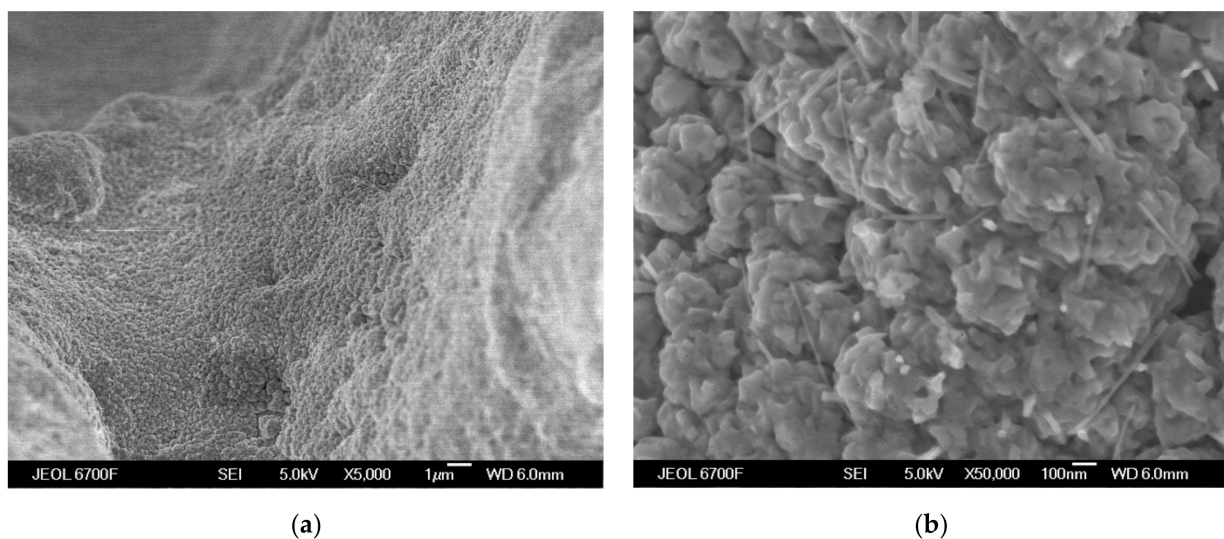

Figure 5. SEM image of the wall of an individual cavity on surface No. 8 at different magnifications. Scale bar: (**a**) 1 μm, 5000 magnification; (**b**) 100 nm, 50,000 magnification.

The contact angle for the smooth copper surface was $54 \pm 2°$, and that for the copper surface with the deposited fluoropolymer was $140 \pm 2°$. The contact angle for the array of micrococoons from silicon oxide nanowires was $36 \pm 2°$, and after fluoropolymer deposition, it was $164 \pm 2°$. For hydrophobized with fluorinated methoxysilane samples, the contact angle was about $170 \pm 2°$ in ablated regions [32]. The roughness R_a of the smooth copper surface was no more than 0.17 μm.

The characterization of the samples was carried out using a JEOL JSM-6700F and a Hitachi S-3400N scanning electron microscopes equipped with energy dispersive X-ray spectrometers (EDS) for element analysis. The water contact angle was measured using a KRUSS DSA-100 device.

2.2. Experimental Setup

The experimental setup is shown schematically in Figure 6 with an indication of the main components. The main component of the setup is a thermostated chamber (see Figures 7 and 8) with five optical windows for monitoring the processes occurring during the experiments. The walls of the chamber are parallel steel plates, between which liquid circulates. The chamber consists of three independent circuits: a box with side walls, an upper wall (lid), and a lower wall (bottom). Each circuit includes a system of connecting pipes and valves and is connected to a thermostat to maintain a uniform and constant temperature distribution on the walls of the chamber. The spatial temperature distribution is monitored by two thermocouples brought into the chamber through a common sealed port and mounted on each wall. The chamber is filled to the required level with the working liquid through the liquid supply channel. At the bottom of the chamber there is a cylindrical working section with a copper core fixed with a special hold-down device. Thermocouples used to measure and calculate the heat flux from the heater are distributed over the working section.
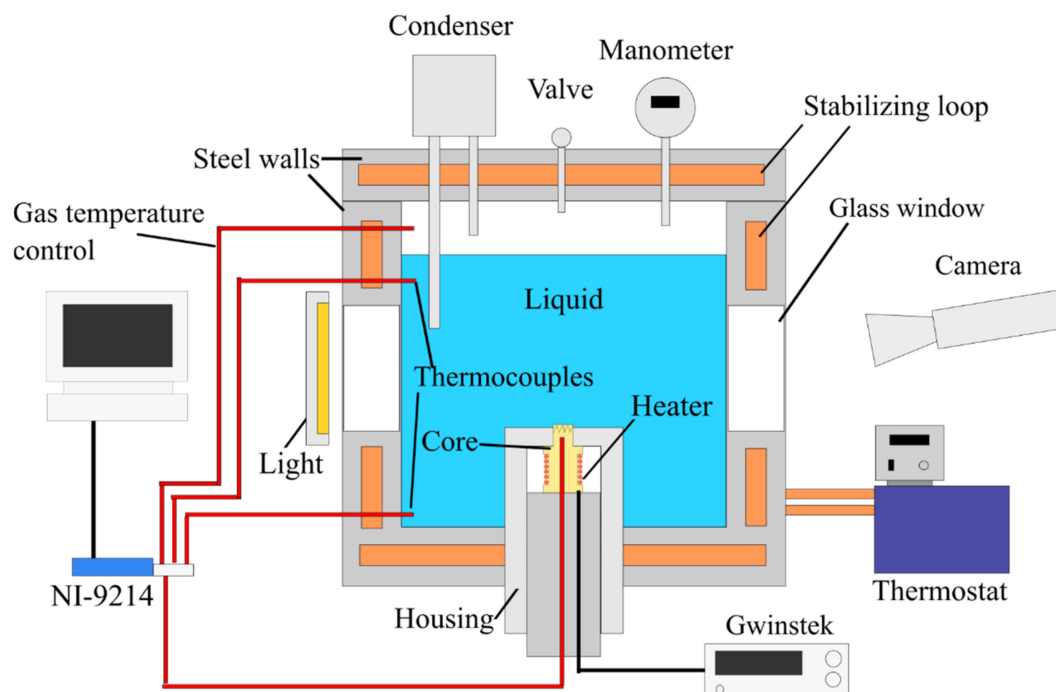

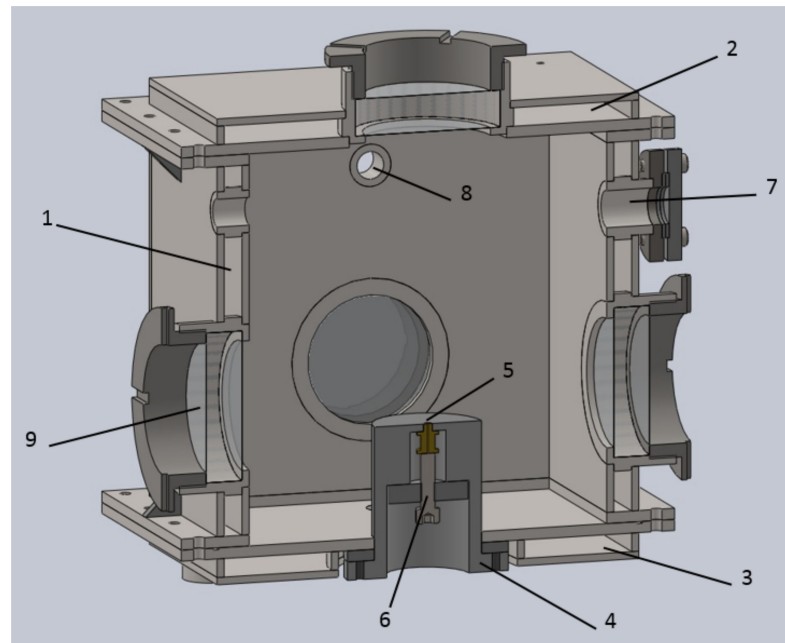**Figure 6.** Sketch of the experimental setup.

Figure 7. View of the thermostated chamber: 1—lateral thermal stabilization circuit, 2—upper thermal stabilization circuit, 3—lower thermal stabilization circuit, 4—working section, 5—heating element, 6—hold-down device, 7—thermocouple entry port, 8—sensor entry port, and 9—optical window.
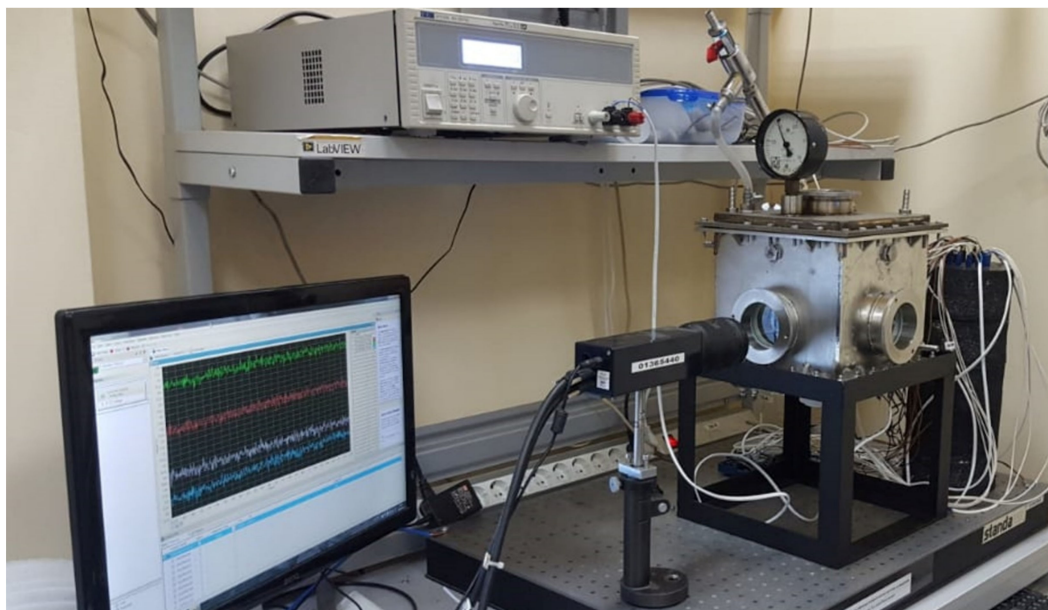

Figure 8. View of the experimental setup.

On the upper wall of the chamber, there is a finned tube steam condenser connected to a cooling circuit with a thermostat. A steam pressure sensor and a pressure relief valve are also located in the upper part of the chamber. A high-speed video camera for high-precision recording of the processes under study is placed opposite the side optical window. An illumination system is mounted on the other side of the thermostated chamber to provide sufficient lighting conditions of the working section during high-speed shooting. An additional general view camera for visualization and monitoring of the experiment is placed above the upper optical window.

The instrument and control system consisted of an NI-9214 data acquisition system and software. The temperature measurement sensitivity of this unit is 0.1 °C. The temperature of the heater, liquid, and environment was measured using thermocouples. Thermocouples were connected with a cold junction (no automatic cold junction compensation) to improve accuracy. The temperature of the heater, liquid, and environment is measured using thermocouples. All thermocouples of the setup were individually calibrated from 0 °C to 150 °C with an interval of 10 °C. A KS 100-1 dry-well calibrator was used below 100 °C, and a Termex VT-8 glycerin thermostat in the range from 100 °C to 150 °C. In both cases, temperature was monitored using a V7-99 meter with ETS-100 resistance thermometers. The calibration error was 0.1 °C. Distilled, deionized, and degassed water (Milli-Q) was used as the working liquid.

The synthesis and deposition of nanocoatings by different methods requires the use of sufficiently small heaters that can be placed in synthesis and deposition chambers, quickly mounted into the setup without damage to the nanostructures on the end heating surface, removed, and regularly monitored with an electron microscope. To perform experiments under the same carefully controlled conditions, it is necessary to fabricate a large series of heaters with identical characteristics.

Comparison of our method with other methods, e.g., gluing silicon wafers with nanostructures to a heater, showed the advantages of the approach used. The heating element is a cylindrical copper core with a head of 5 mm diameter (Figure 9). The boiling surface is the flat top end of the cylinder. The tip of the core is tightly inserted into the hole of the fluoropolymer base and is aligned in one plane with the top of the base. The heat source is a Nichrome wire tightly wound around the core stem with a resistance of 4 Ohm. The heating element is carefully insulated to minimize heat loss. Glass fabric wrapped in several layers around the core of the heating element is used as a heat insulator.
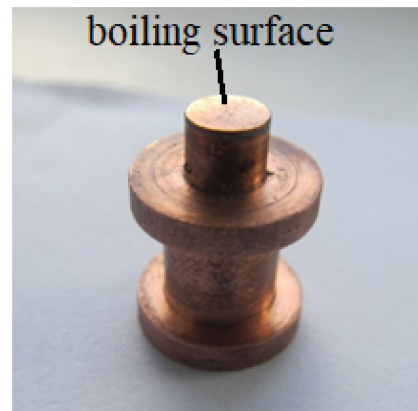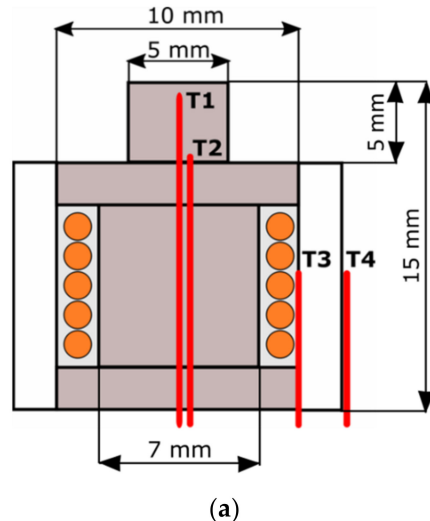

(**a**)   (**b**)

Figure 9. Sketch (**a**) and photo (**b**) of the typical heating element (photo was created before modifications).

Two thermocouples T1 and T2 were mounted in grooves at different depths in the copper core (Figure 9) to measure the surface temperature and determine the heat flux according to the Fourier law. To monitor the heat flux distribution, additional thermocouples T3 and T4 were mounted in the region of the core and used for winding the Nichrome heater.

The heat flux supplied to the test section was calculated by Fourier's law [33] as:

$$q = -k_{Cu} \frac{T2 - T1}{X1} \tag{1}$$

where q is the heat flux, $X1$ is the distance between thermocouples $T2$ and $T1$, and k_{Cu} is the thermal conductivity of copper.

The surface temperature was determined from the equation [33]:

$$T_w = T1 - q \left(\frac{X2}{k_{Cu}} \right) \qquad (2)$$

where T_w is the temperature of the test surface and $X2$ is the distance between the test surface and thermocouple $T1$.

The main source of the measurement error was inaccuracy in determining the real heat flux. This inaccuracy is due to the calibration error of thermocouples $T1$ and $T2$, the error in determining the depth of grooves for thermocouple placement, and the inaccuracy of their positioning in the grooves. The calibration error was 0.1 °C, as already mentioned above. The total positioning error of the thermocouples was about 0.01 mm. The measurement error was estimated using the well-known formulas mentioned in [33]. The final error of temperature determination was no more than 0.2 °C. The heat flux error did not exceed 3 W/cm^2.

3. Results

3.1. Validation of the Experimental Setup and Measurement Technique

Before the main experiments, a series of test measurements was performed on smooth copper surfaces. The results of the series for the three experiments of pool boiling on smooth copper are shown in Figure 10.
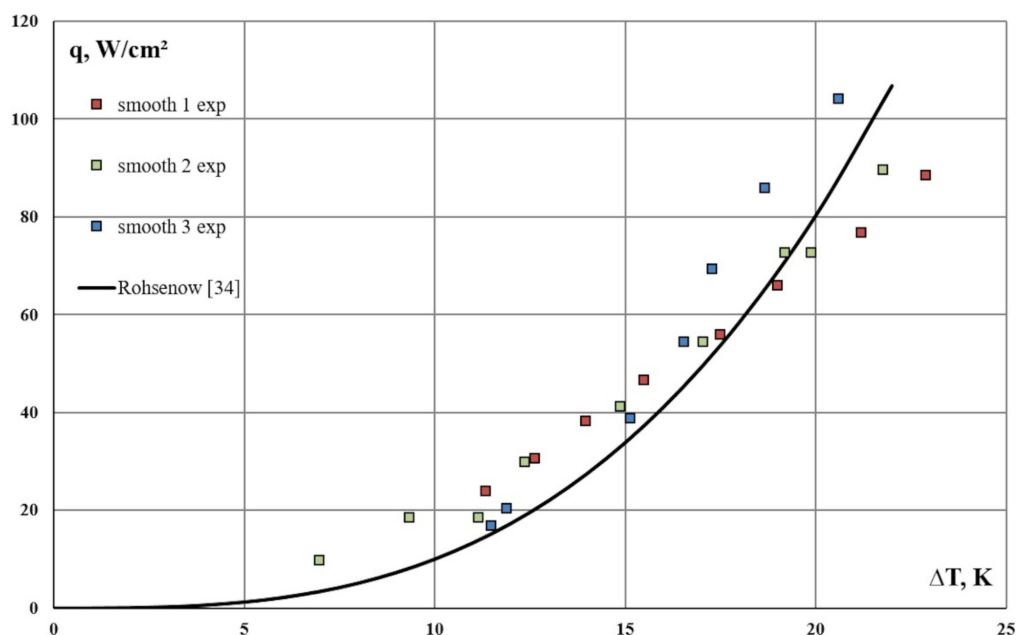

Figure 10. Dependence of the heat flux on the temperature difference between the heating surface and the liquid under saturation conditions for the smooth surface.

The well-known Rohsenow correlation [34] was used for comparison. For the correlation, the coefficients for surfaces with the closest characteristics were used. The data are in good agreement with the theoretical curve. The average deviation does not exceed 15%. The second experiment has the least standard deviation (8 W/cm^2) from the theoretical curve. These results exceed the previously calculated experimental errors but this can be explained by the incompletely matched surface parameters (roughness, degree of oxidation). Thus, the experimental setup and the measurement technique can be considered valid and to provide reliable results. Further, all experimental results are compared with the Rohsenow correlation.

3.2. Experimental Results

The effect of the size of round hydrophobic spots and the pitch between them on the boiling heat transfer rate was studied. In the first series of experiments, surfaces with hydrophobic fluoropolymer regions 100 μm in diameter and a pitch of 500 μm were used. A boiling curve was first obtained for a smooth copper surface with fluoropolymer spots (surface No. 4). The result is shown in Figure 11. It can be seen from the figure that the heat transfer on the biphilic surface is enhanced compared to the homogeneous smooth copper surface (Rohsenow correlation). A similar result was obtained for surfaces covered with arrays of micrococoons: boiling heat transfer on surfaces No. 2 and No. 3 with fluoropolymer spots is more intense than on surface No. 1 (a homogeneous array of micrococoons without hydrophobic spots). Note that the results for surfaces No. 2 and No. 3 are approximately the same, which indicates that the technology is reproducible. Thus, biphilicity enhances heat transfer on both smooth surfaces and surfaces covered with micrococoons from silicon oxide nanowires. It is additionally notable that the results on smooth surface No. 4 are slightly superior to the results on surfaces No. 2 and No. 3, despite the initial assumption that pre-coating with micrococoons would enhance boiling heat transfer on the biphilic surface.
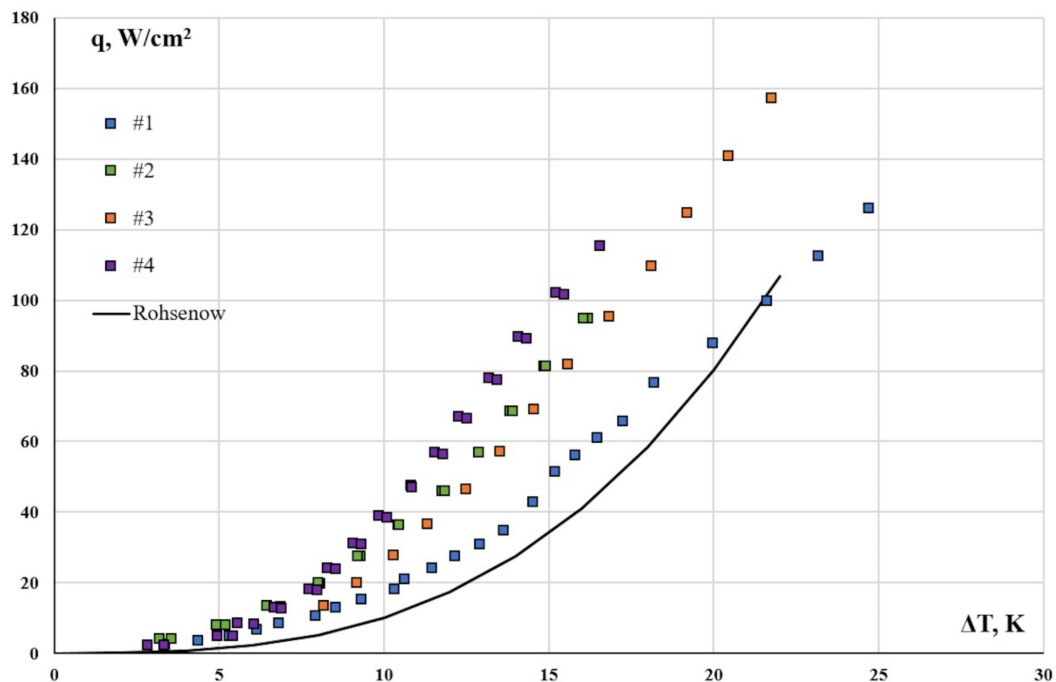

Figure 11. Boiling curves for surface No. 1 and surfaces Nos. 2–4 from Table 1 with deposited fluoropolymer spots 100 μm in diameter with a pitch of 500 μm.

Surfaces with hydrophobic fluoropolymer regions 50 μm in diameter with a pitch of 200 μm exhibit a similar behavior in experiments (Figure 12). The heat transfer performance of smooth copper surface No. 6 with hydrophobic spots is higher than that of surface No. 5 covered with arrays of micrococoons with hydrophobic spots. However, in this case, the effect is much less pronounced and is observed at heat fluxes of about 60 to 130 W/cm^2.
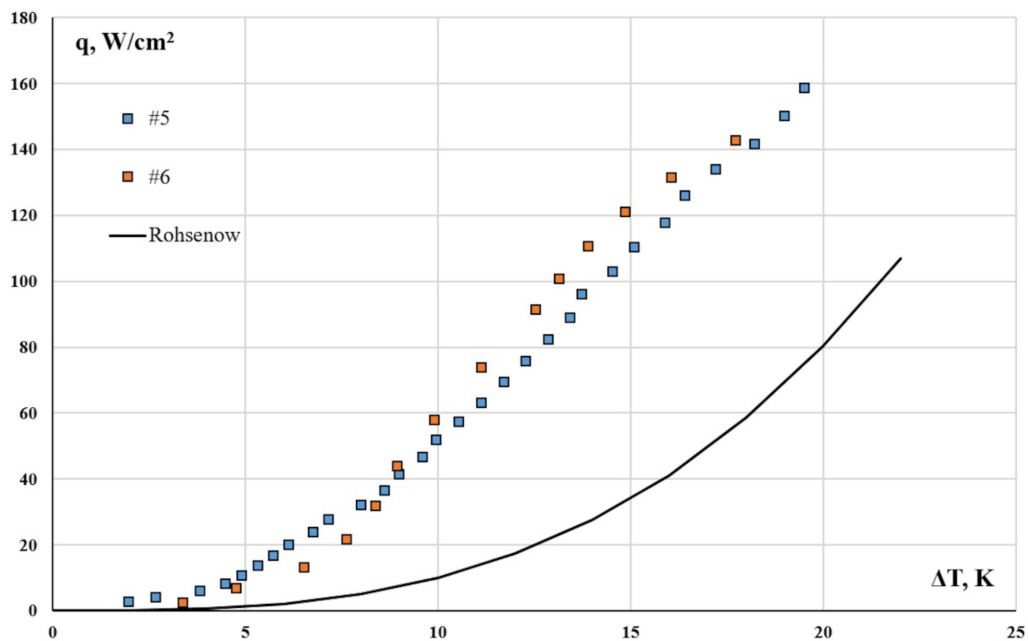
Figure 12. Boiling curves for surface Nos. 5 and 6 from Table 1 with deposited fluoropolymer spots 50 μm in diameter with a pitch of 200 μm.

A comparison of the efficiency of using surfaces with fluoropolymer spots 100 μm in diameter with a pitch of 500 μm and surfaces with spots 50 μm in diameter with a pitch of 200 μm shows a fairly significant increase of up to 20% in heat transfer rate for surfaces with smaller spots and a smaller pitch. Moreover, this effect is observed both for surfaces with arrays of micrococoons (Nos. 2, 3, and 5) (Figure 13) and for smooth copper surfaces (Nos. 4 and 6) (Figure 14).
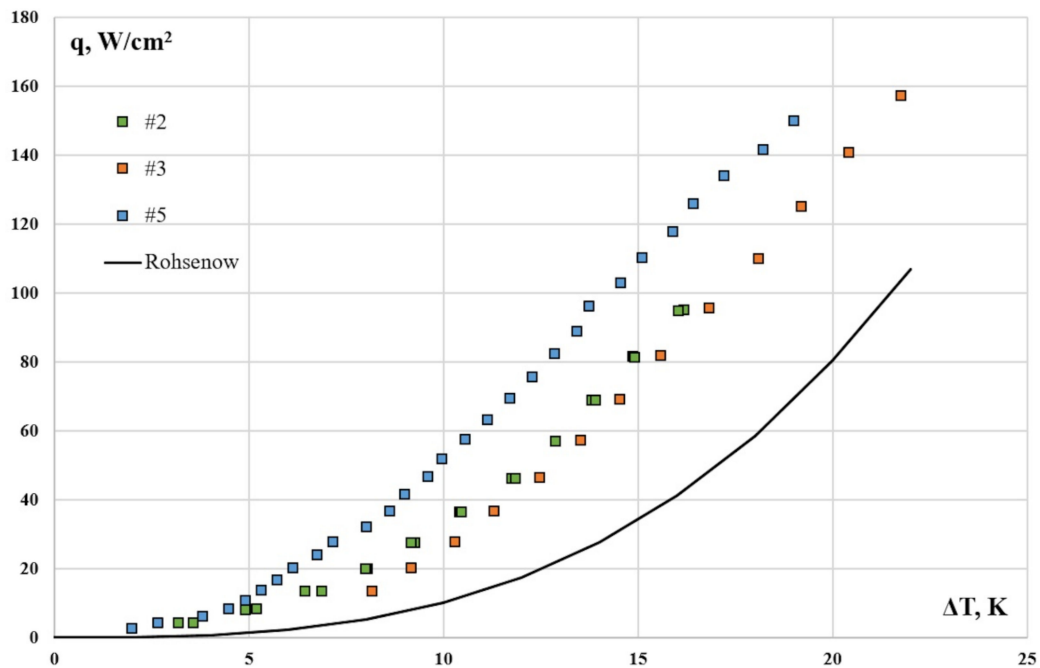

Figure 13. Comparison of boiling curves for surfaces Nos. 2 and 3 (spot diameter 100 μm, pitch 500 μm) and surface No. 5 (spot diameter 50 μm, pitch 200 μm) with arrays of micrococoons.
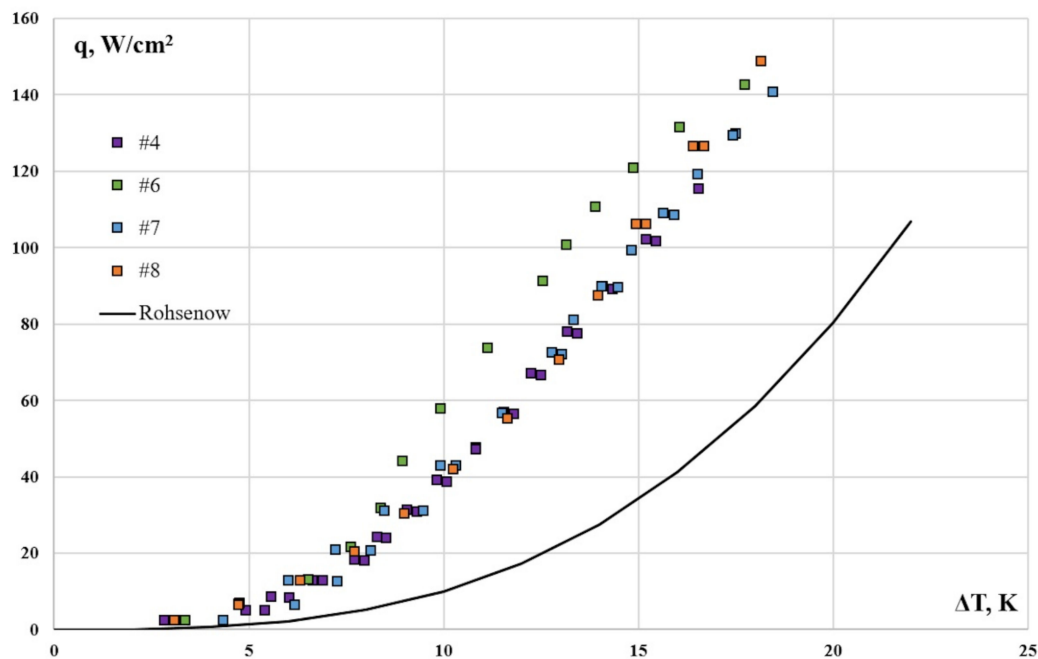
Figure 14. Boiling curves for surfaces Nos. 4, 6, 7, and 8.

Figure 14 shows data for surfaces No. 4 (spot diameter 100 μm, pitch 500 μm), No. 6 (spot diameter 50 μm, pitch 200 μm), and for surfaces Nos. 7 and 8 (triangular and rectangular cavities, respectively) obtained by laser methods.

It can be seen that the heat transfer rate on surface No. 6 is 20% higher than on the other surfaces, including surface No. 4. Thus, in view of the data in Figure 13, it can be concluded that for all biphilic samples with fluoropolymer spots of 50 μm in diameter and a pitch of 200 μm, the heat transfer efficiency is higher than for samples with spots of 100 μm in diameter and a pitch of 500 μm.

4. Discussion

4.1. Effect of Surface Properties on Boiling

All biphilic surfaces show an intensity of heat transfer that is more than twice as high (up to 600%) as a smooth copper surface. Heat transfer intensification on surfaces obtained using a 50/200 mask (Nos. 5 and 6) is 20% higher than on the other surfaces.

Biphilic surfaces Nos. 7 and 8 are most comparable in the spot area (in the plane of the surface) and spot pitch to surface No. 4. The heat transfer rates on these three surfaces are almost identical, although their shape, texture, and depth of cavities are significantly different. Apparently, the initial assumption that the hydrophobic layer is rapidly destroyed on the main surface and has good stability in cavities obtained by ablation turns out to be valid.

It was already mentioned above that the boiling heat transfer rate on biphilic surfaces is significantly affected by the following factors: the size of hydrophobic spots, the distance between them (pitch), and the area ratio (the ratio of the total hydrophobic surface area to the total boiling area). A significant difference of surface No. 6 is that it has a much larger (by an order of magnitude) number of hydrophobic spots: 506 versus 69 for surface No. 4 and 32 for surfaces No. 7 and No. 8. The larger area ratio for surface No. 6 (5.1%) compared to the area ratio for surfaces No. 4 (2.8%), No. 7 (2.1%), and No. 8 (3.4%) may also affect the heat transfer enhancement.

It can be assumed that the use of a small number of large spots is indeed less effective since closely spaced vaporization centers in the same spot interfere with each other, and it is worth isolating them from each other by reducing the spot size in parallel with decreasing

the spot pitch. However, in general, the question of the optimal characteristics of biphilic surfaces remains open and requires further detailed study.

4.2. Comparison with Literature Data

A review of the literature showed that the available data on pool boiling of water on flat copper heaters at atmospheric pressure are few in number. Systemic data on the optimal geometry of hydrophobic regions and the optimal area ratio are absent or inconsistent. A comparison with the results of the studies cited above is shown in Figure 15. It can only be noted that our data on the degree of hydrophobicity are closest to those reported in the paper by Yamada et al. [18], where hydrophobic regions occupy approximately 2.2%. It can be seen that the data obtained for some of the most characteristic surfaces (Nos. 4, 6, and 8) are superior to the results of Yamada.
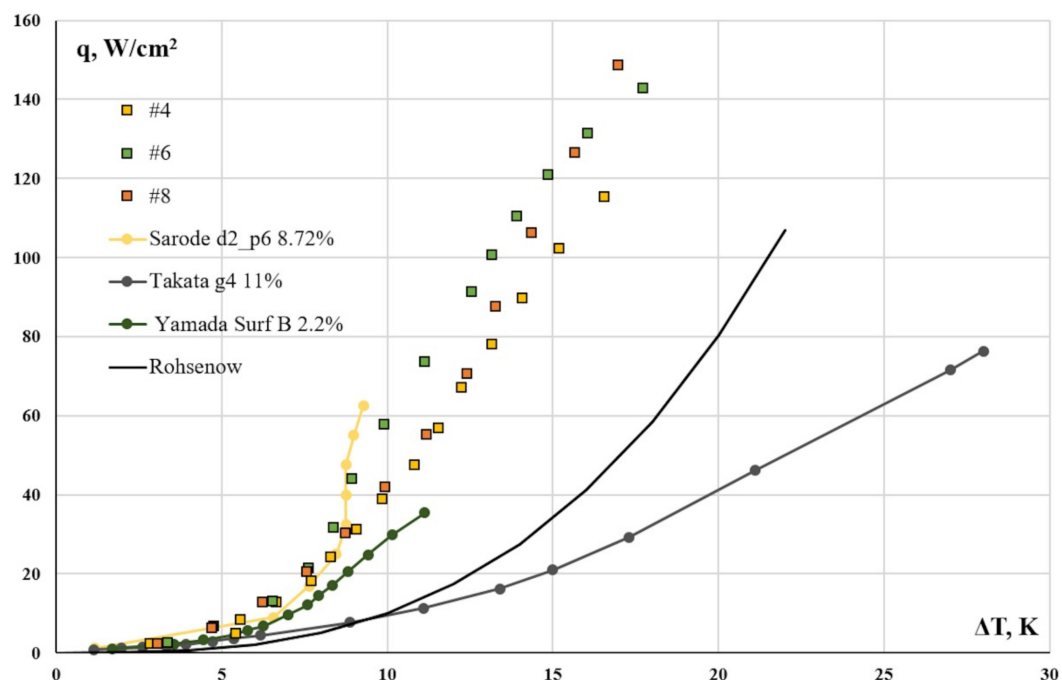

Figure 15. Boiling curves for surfaces Nos. 4, 6, and 8 and some literature data.

4.3. Stability of the Biphilic Surfaces

An important problem in the operation of various micro/nanomodified surfaces is their aging. During operation, many surfaces undergo morphological changes that can be associated with mechanical destruction by boiling due to the effect of growing bubbles on micro/nanostructures and/or due to different thermal expansion coefficients of surface materials during layer-by-layer deposition of films of several materials. In addition, intense hydrothermal loads can cause chemical changes on surfaces.

In the literature, insufficient attention is paid to these issues and there is no mention of the reproducibility of experiments.

In this work, we performed a series of long-term (two-year) experiments for surfaces Nos. 7 and 8 (with cavity microstructures formed by laser ablation), in which samples of these surfaces demonstrated high stability. As an example, Figure 16 shows boiling curves for surface No. 7 measured on different dates. It can be seen from these data that the pool boiling heat transfer rate of the surface remains high throughout the period of operation and the boiling curves do not show significant changes.
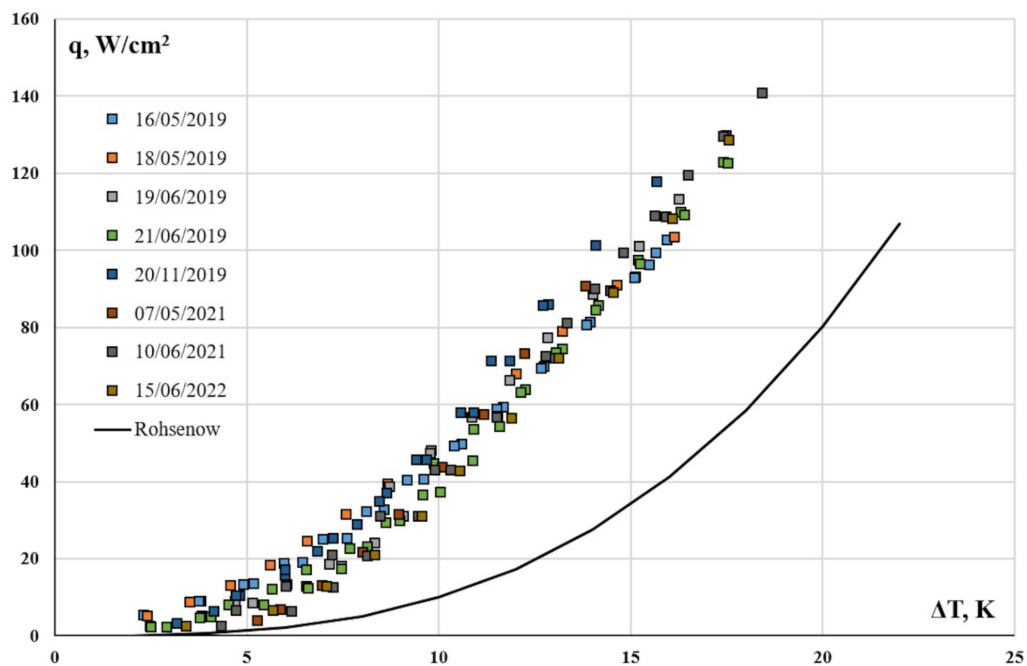
Figure 16. Boiling curves for surface No. 7 showing its stability. DD/MM/YYYY format was used.

Surfaces obtained by local deposition of the fluoropolymer through a mask onto smooth copper did not exhibit high stability compared to surfaces No. 7 and No. 8. As an example, Figure 17 shows some data for surface No. 4. After the best result obtained on 7 June 2019, the heat transfer rate decreased in the subsequent experiments.
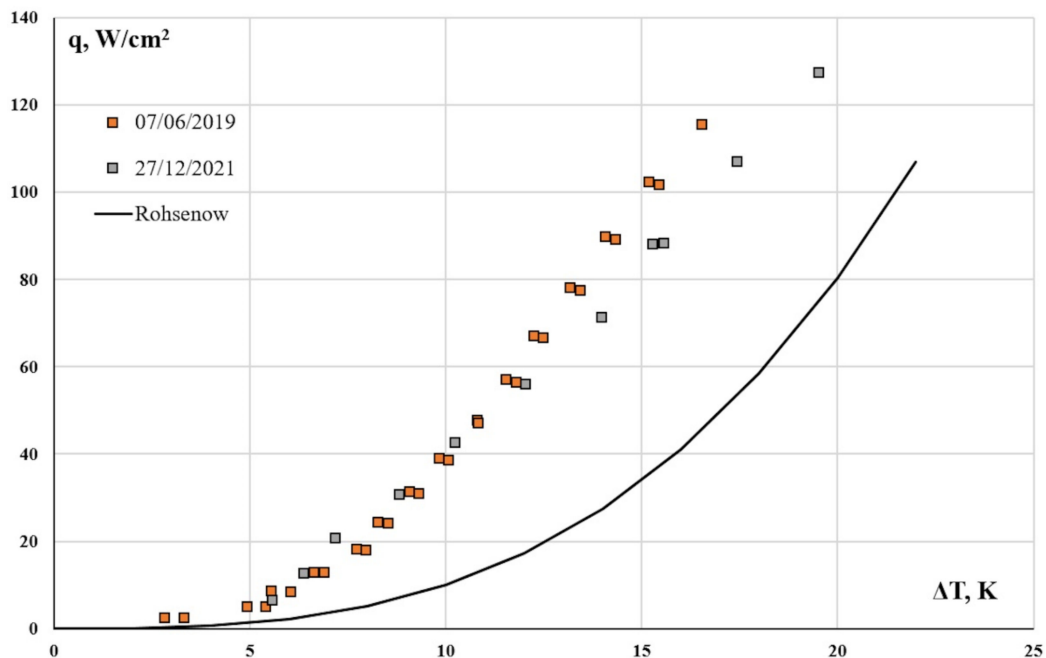

Figure 17. Boiling curves for surface No. 4.

Surfaces obtained by local deposition of the fluoropolymer on an array of micrococoons also did not exhibit high stability, despite the initial assumptions that the adhesion of the fluoropolymer deposited on microstructures would be higher than in the case of deposition on smooth copper. Some data for surface No. 3 are given in Figure 18. Just as for surface No. 4, the heat transfer rate decreased after the first experiments.
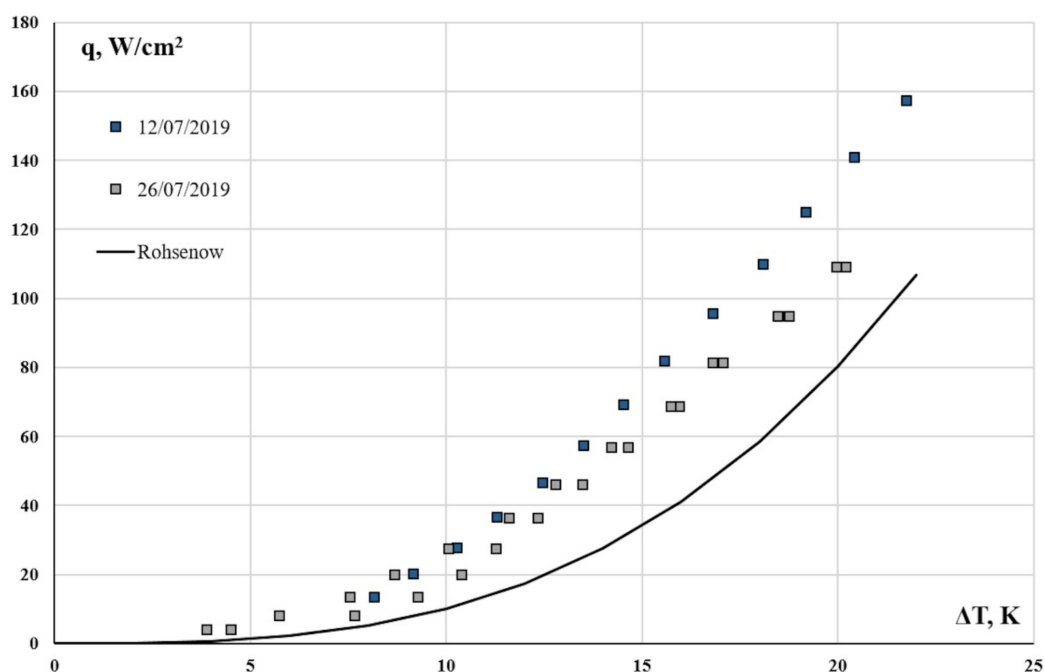
Figure 18. Boiling curves for surface No. 3.

The standard deviations between the experimental curves in both cases exceed 11 W/cm^2, which is much larger than the experimental error.

5. Conclusions

1. Boiling experiments were carried out using two types of biphilic surfaces obtained by different techniques. The degrees of heat transfer enhancement on nano-modified surfaces were determined. The effect of the size (0.05, 0.07, 0.1 mm), shape (circle, triangular, rectangular), and number of hydrophobic spots (32 to 506) on the boiling heat transfer rate on eight copper surfaces was studied.

2. Both techniques demonstrated their effectiveness and provided a significant enhancement of boiling heat transfer. The heat transfer coefficient on biphilic surfaces was significantly (up to 600 %) higher than on smooth surfaces or surfaces coated with cocoons.

3. The boiling heat transfer rate depended on the size of hydrophobic spots, the distance between them, and hence on their number. The results complement previous data [7,18] and show that heat transfer enhancement can be obtained on surfaces with a small diameter of hydrophobic regions (0.05 mm) and a relatively small area ratio (5%). At the same time, no significant effect of surface texture and shape of hydrophobic regions tested in this study on heat transfer was found.

4. After long-term experiments (over 1 to 3 years), the heat transfer coefficient on the obtained surfaces remained higher than on a smooth copper surface. During 3 years of operation, the best stability of enhanced heat transfer was observed for biphilic surfaces with cavities formed by laser ablation.

Institutional Review Board Statement: Not applicable.

Informed Consent Statement: Not applicable.

Data Availability Statement: Not applicable.

Conflicts of Interest: The authors declare no conflict of interest. The funders had no role in the design of the study; in the collection, analyses, or interpretation of data; in the writing of the manuscript; or in the decision to publish the results.

Nomenclature

q—heat flux, W/cm^2; k_{Cu}—thermal conductivity of copper, W/(m*K); T—temperature, K, °C; X—distance, mm; Contact angle, °.

References

1. Liang, G.; Mudawar, I. Review of pool boiling enhancement by surface modification. *Int. J. Heat Mass Transf.* **2019**, *128*, 892–933. [CrossRef]
2. Li, W.; Dai, R.; Zeng, M.; Wang, Q. Review of two types of surface modification on pool boiling enhancement: Passive and active. *Renew. Sustain. Energy Rev.* **2020**, *130*, 109926. [CrossRef]
3. Chen, J.; Ahmad, S.; Cai, J.; Liu, H.; Lau, K.T.; Zhao, J. Latest progress on nanotechnology aided boiling heat transfer enhancement: A review. *Energy* **2021**, *215*, 119114. [CrossRef]
4. Kamel, M.S.; Lezsovits, F.; Hussein, A.K. Experimental studies of flow boiling heat transfer by using nanofluids A critical recent review. *J. Therm. Anal. Calorim.* **2019**, *138*, 4019–4043. [CrossRef]
5. Surtaev, A.S.; Serdyukov, V.S.; Pavlenko, A.N. Nanotechnologies for thermophysics: Heat transfer and crisis phenomena at boiling. *Nanotech. Russia* **2016**, *11*, 696–715. [CrossRef]
6. Dedov, A.V. A Review of Modern Methods for Enhancing Nucleate Boiling Heat Transfer. *Therm. Eng.* **2019**, *66*, 881–915. [CrossRef]
7. Serdyukov, V.; Patrin, G.; Malakhov, I.; Surtaev, A. Biphilic surface to improve and stabilize pool boiling in vacuum. *Appl. Therm. Eng.* **2022**, *209*, 118298. [CrossRef]
8. Motezakker, A.R.; Sadaghiani, A.K.; Çelik, S.; Larsen, T.; Villanueva, L.G.; Koşar, A. Optimum ratio of hydrophobic to hydrophilic areas of biphilic surfaces in thermal fluid systems involving boiling. *Int. J. Heat Mass Transf.* **2019**, *135*, 164–174. [CrossRef]
9. Hummel, R.L. Means for Increasing the Heat Transfer Coefficient between a Wall and Boiling Liquid. U.S. Patent No. 3207209, 21 September 1965. Available online: https://patents.google.com/patent/US3207209A/en (accessed on 5 July 2022).
10. Attinger, D.; Frankiewicz, C.; Betz, A.R.; Schutzius, T.M.; Ganguly, R.; Das, A.; Kim, C.-J.; Megaridis, C.M. Surface engineering for phase change heat transfer: A review. *MRS Energy Sustain.* **2014**, *1*, 4. [CrossRef]
11. Betz, A.R.; Xu, J.; Qiu, H.; Attinger, D. Do surfaces with mixed hydrophilic and hydrophobic areas enhance pool boiling? *Appl. Phys. Lett.* **2010**, *97*, 141909. [CrossRef]
12. Jo, H.; Ahn, H.S.; Kang, S.; Kim, M.H. A study of nucleate boiling heat transfer on hydrophilic, hydrophobic and heterogeneous wetting surfaces. *Int. J. Heat Mass Transf.* **2011**, *54*, 5643–5652. [CrossRef]
13. Betz, A.R.; Jenkins, C.-J.; Kim, C.-J.; Attinger, D. Boiling heat transfer on superhydrophilic, superhydrophobic, and superbiphilic surfaces. *Int. J. Heat Mass Transf.* **2013**, *57*, 733–741. [CrossRef]
14. Jo, H.J.; Kim, S.H.; Park, H.S.; Kim, M.H. Critical heat flux and nucleate boiling on several heterogeneous wetting surfaces: Controlled hydrophobic patterns on a hydrophilic substrate. *Int. J. Multiph. Flow* **2014**, *62*, 101–109. [CrossRef]
15. Colombo, L.; Alberti, L.; Mazzon, P.; Antelmi, M. Null-space Monte Carlo particle backtracking to identify groundwater tetrachloroethylene sources. *Front. Environ. Sci.* **2020**, *8*, 142. [CrossRef]
16. Wenzel, R.N. Resistance of solid surfaces to wetting by water. *Ind. Eng. Chem.* **1936**, *28*, 988–994. [CrossRef]
17. Takata, Y.; Hidaka, S.; Kohno, M. Effect of surface wettability on pool boiling: Enhancement by hydrophobic coating. *Int. J. Air-Cond. Refrig.* **2012**, *20*, 1150003. [CrossRef]
18. Yamada, M.; Shen, B.; Imamura, T.; Hidaka, S.; Kohno, M.; Takahashi, K.; Takata, Y. Enhancement of boiling heat transfer under sub-atmospheric pressures using biphilic surfaces. *Int. J. Heat Mass Transf.* **2017**, *115*, 753–762. [CrossRef]
19. Sarode, A.; Raj, R.; Bhargav, A. Scalable macroscale wettability patterns for pool boiling heat transfer enhancement. *Heat Mass Transf.* **2020**, *56*, 989–1000. [CrossRef]
20. Liang, G.; Chen, Y.; Wang, J.; Wang, Z.; Shen, S. Experiments and modeling of boiling heat transfer on hybrid-wettability surfaces. *Int. J. Multiph. Flow* **2021**, *144*, 103810. [CrossRef]
21. Može, M.; Zupančič, M.; Golobič, I. Pattern geometry optimization on superbiphilic aluminum surfaces for enhanced pool boiling heat transfer. *Int. J. Heat Mass Transf.* **2020**, *161*, 120265. [CrossRef]
22. Xia, Y.; Gao, X.; Li, R. Surface effects on sub-cooled pool boiling for smooth and laser-ablated silicon surfaces. *Int. J. Heat Mass Transf.* **2022**, *194*, 123113. [CrossRef]

23. Zupančič, M.; Steinbücher, M.; Gregorčič, P.; Golobič, I. Enhanced pool-boiling heat transfer on laser-made hydrophobic/superhydrophilic polydime thylsiloxane-silica patterned surfaces. *Appl. Therm. Eng.* **2015**, *91*, 288–297. [CrossRef]

24. Može, M. Effect of boiling-induced aging on pool boiling heat transfer performance of untreated and laser-textured copper surfaces. *Appl. Therm. Eng.* **2020**, *181*, 116025. [CrossRef]

25. Khmel, S.; Baranov, E.; Vladimirov, V.; Safonov, A.; Chinnov, E. Experimental study of pool boiling on heaters with nanomodified surfaces under saturation. *Heat Transf. Eng.* 2021. Available online: https://www.tandfonline.com/doi/full/10.1080/01457632.2 021.2009211(accessed on 5 July 2022).

26. Cho, H.R.; Park, S.C.; Kim, D.; Joo, H.-m.; Yu, D.I. Experimental study on pool boiling on hydrophilic micro/nanotextured surfaces with hydrophobic patterns. *Energies* **2021**, *14*, 7543. [CrossRef]

27. Freitas, E.; Pontes, P.; Cautela, R.; Bahadur, V.; Miranda, J.; Ribeiro, A.P.C.; Souza, R.R.; Oliveira, J.D.; Copetti, J.B.; Lima, R.; et al. Pool boiling of nanofluids on biphilic burfaces: An experimental and numerical study. *Nanomaterials* **2021**, *11*, 125. [CrossRef]

28. Boinovich, L.B.; Emelyanenko, A.M. The behaviour of fluoro-and hydrocarbon surfactants used for fabrication of superhydrophobic coatings at solid/water interface. *Coll. Surf. A Phys. Eng. Asp.* **2015**, *481*, 167–175. [CrossRef]

29. Boinovich, L.B.; Emelyanenko, K.A.; Domantovsky, A.G.; Chulkova, E.V.; Shiryaev, A.A.; Emelyanenko, A.M. Pulsed laser induced triple layer copper oxide structure for durable polyfunctionality of superhydrophobic coatings. *Adv. Mater. Interfaces* **2018**, *5*, 1801099. [CrossRef]

30. Safonov, A.I.; Sulyaeva, V.S.; Gatapova, E.Y.; Starinskiy, S.V.; Timoshenko, N.I.; Kabov, O.A. Deposition features and wettability behavior of fluoropolymer coatings from hexafluoropropylene oxide activated by NiCr wire. *Thin Solid Films* **2018**, *653*, 165–172. [CrossRef]

31. Chinnov, E.A.; Shatskiy, E.N.; Khmel, S.Y.; Baranov, E.A.; Zamchiy, A.O.; Semionov, V.V.; Kabov, O.A. Enhancement of heat transfer at pool boiling on surfaces with silicon oxide nanowires. *J. Phys. Conf. Series* **2017**, *925*, 012033. [CrossRef]

32. Vladimirov, V.Y.; Khmel, S.Y.; Safonov, A.I.; Semionov, V.V.; Chinnov, E.A. Effect of fluoropolymer spots on pool boiling heat transfer. *J. Phys. Conf. Series* **2021**, *2119*, 012087. [CrossRef]

33. Može, M.; Zupančič, M.; Golobič, I. Investigation of the scatter in reported pool boiling CHF measurements including analysis of heat flux and measurement uncertainty evaluation methodology. *App. Therm. Eng.* **2020**, *169*, 114938. [CrossRef]

34. Rohsenow, W.M. *A Method of Correlating Heat Transfer Data for Surface Boiling of Liquids*; Technical Report No 5 (Heat Transfer Laboratory); MIT Division of Industrial Cooperation: Cambridge, MA, USA, 1951. Available online: https://dspace.mit.edu/handle/1721.1/61431 (accessed on 5 July 2022).